Tsunami hazard assessment in the Ionian Sea due to potential tsunamogenic sources - Results from numerical simulations

G-A. Tselentis[(1)], G. Stavrakakis[(2)], E. Sokos[(1)], F. Gkika[(1)] and A. Serpetsidaki[(2)]

(1) University of Patras, Seismological Lab.

(2) National Observatory of Athens, Geodynamic Institute.

Abstract

In spite of the fact that the great majority of seismic tsunami is generated in ocean domains, smaller basins as the Ionian Sea sometimes experience this phenomenon. In this investigation we study the tsunami hazard associated with the Ionian Sea fault system.

A scenario-based method is employed to provide an estimation of tsunami hazard in this region for the first time. Realistic faulting parameters related to four probable seismic sources with tsunami potential are used to model expected coseismic deformation, which is translated directly to the water surface and used as an initial condition for the tsunami propagation.

We calculate tsunami propagation snapshots and mareograms for the four seismic sources in order to estimate the expected values of tsunami maximum amplitudes and arrival times at eleven tourist resorts along the Ionian shorelines.

The results indicate that from the four examined sources only one possesses seismic threat causing, wave amplitudes up to 4m at some tourist resorts along the Ionian shoreline.

Introduction

The western part of the Hellenic arc is one of the most seismically active areas in Greece and the entire Mediterranean region (Makropoulos and Burton 1981; Jackson and McKenzie 1988; Papazachos and Papazachou 1997). This area has been repeatedly affected by large magnitude earthquakes (Fig. 1) that have caused severe destruction and human loss.

Large tsunami events require the presence of a thick water layer that can be found only in the oceanic domain but it can also occur in small basins, as the Ionian Sea, where many tsunamis have been reported during historical times.

The Ionian region has an unexpected economic and tourist growth with an increase in coastal population and the development of large leisure areas during recent years, with many parts of coastal cities being a couple of meters above sea level, making them prospective targets to suffer a large-scale disaster, even if the height of the tsunami wave is moderate. This situation requires urgent solutions for an effective risk management and mitigation plan. For this reason it is essential to define the tsunami potential of the region and this study present the first results of such an attempt.

The lack of direct records however, makes a rigorous estimation of the expected tsunami amplitudes rather difficult, and the analysis of available documents remains somehow controversial.

Any attempt to assess tsunami hazard based on pure statistical methodologies will not give reliable results because of data deficiency, and because they use relationships linking earthquakes to tsunamis that may not be empirically well grounded. This means that alternative approaches to evaluate tsunami hazard are to be invoked (e.g.Tselentis et al., 2006). Most often, a solution to the problem is searched for, in terms of a scenario that is considering the largest events known to have hit the area of interest in the past history and to simulate these events through numerical modeling.

This is the approach used in the present investigation, focusing on the tectonic deformation mechanics of the potential tsunamigenic faults and their effect on the tsunami hazard in the region.

Tectonic setting and Tsunamigenic Environment

Western Greece, (Ionian Islands and Western Peloponnese), represents one of the most seismotectonically active regions of the Mediterranean. The Aegean is a region of intense deformation located between two major lithospheric plates, the European plate and the African plate The African plate is moving northwards relative to Eurasia at a rate of 10 mm/year (DeMets et al., 1990), and its leading edge is being subducted along the Hellenic Trench.

Seismological investigations (Jackson 1994) and geodesy (Noomen et al., 1995) reveal that the relative motion across the Hellenic trench is NE-SW and greater than 5 cm/yr, while GPS measurements (Kahle et al., 1993) show a distinct movement of western Greece to the SW relative to Italy with an average of 120 mm between 1989 and 1993.

Seismotectonics of western Greece has been extensively studied (e.g. Haslinger et al., 1999). The major tectonic features, which set the Ionian Sea as an area of high seismicity are: the subduction of the African plate beneath the Aegean microplate along the western Hellenic trench, and the Cephallonia transfer fault at the northwestern end of the Hellenic arc, which is a major strike-slip fault that links the subduction boundary to the continental collision between the Apulian microplate and the Hellenic foreland.

Fault plane solutions for several shallow and intermediate depth earthquakes in the Hellenic arc have been published (Taymaz et al., 1990; Papazachos et al., 1991); Their results indicate that in the western part of the Hellenic arc, the thickness of the shallow seismogenic layer covers the upper 20km of the crust. The area extending from Zakynthos to Messinia is extensional, limited by two main fault zones, the one striking NE-SW, offshore Kyllini, dipping to the south east, and the other striking EW, offshore Pylos, dipping to the north. According to Mariolakos et al. (1985) and Papanikolaou et al. (2007) these fault zones are active, and are the offshore extensions of EW trending faults of Western Peloponnese.

Western Greece, has been repeatedly suffered large offshore earthquakes (i.e. 1886 Philiatra M7.3, 1893 Zakynthos-Keri M6.5, 1899 Kyparissia M6.5, 1947 Pylos M7.0, and 1997 Gargaliani M6.6), which have caused damage and human loss (Papazachos and Papazachou, 1997). The presence of tsunamis has been observed a few times in the past, associated with offshore earthquakes (i.e. 1633 and 1886), affecting near field as well as remote coastal segments (Table 1).

Damage was minor from these events, due to the sparse population of the region in the early years. Today, a large earthquake along the Ionian sea fault system would damage coastal communities, and its effect would be enhanced by sea waves triggered from the seafloor displacement.

Taking into account the Ionian Sea tectonic regime and the tsunamogenic events depicted in Table 1, we have selected four potential seismic sources that could represent tsunami hazard in the region (Fig.1). The geographic location, strike, length and other parameters of each source were derived from existing fault maps, available reflection profiles and relevant seismological references and are presented in Table 2.

Elastic Dislocation Modeling

The traditional approach to model tsunami generation is based on solving the hydrodynamic equations with boundary conditions at the seafloor corresponding to a static displacement caused by the earthquake source (e.g. Okal 1982, Comer 1984).

Offshore shallow earthquakes result in a seafloor coseismic deformation that can trigger a tsunami. Most studies of earthquake generated tsunamis use Mansinha and Smylie's (1971) formula or Okada's (1985) analytical formula based on elastic dislocation theory to predict seafloor displacement due to an earthquake and to model initial water displacement (e.g. Legg et al., 2004; Tselentis et al., 2006). This approach is being adopted and in the present investigation.

In general, we assume that this coseismic deformation is much more rapid than the characteristic time involved in the wave propagation, and that the length scale of the seafloor deformation is much larger than the water depth. This, allows us to define the initial subsurface deformation as being equal to the coseismic vertical displacement.

Table 2 presents the source models of the selected tsunamigenic sources used in the present study. The corresponding fault slips u, were determined from (Papazachos and Papazachou, 1997)

$$\text{Log}u=0.82M-3.71 \tag{1}$$

Where M is the magnitude.

Initial conditions for tsunami propagation from all three selected potential seismic sources are determined from the static displacement field by using the three-dimensional elastic boundary element method algorithm POLY-3D (Thomas, 1993), assuming a Poisson's ratio of 0.25.

Next, we calculate the sea-bottom strain field for each one of the four fault scenarios considering the source characteristics depicted in Table 2. The obtained results are shown in Fig.2, and the corresponding vertical displacements are presented in Table 3.

Calculations of seafloor displacements are made assuming a homogeneous elastic structure (Poisson's solid). The effect of elastic inhomogeneity on surface displacements and tsunami waveforms is not included in this study. The near shore tsunami amplitude values predicted in this investigation ignore the possibility of large submarine landslides being triggered by the earthquake, and this study focuses on the tectonic sources only.

Tsunami Modeling

The deformation field, obtained above, is used as an initial condition of the hydrodynamic computation. This constitutes a legitimate approximation since the deformation of the seafloor always takes place much more rapidly than the tsunami waves can propagate the sea surface deformation away from the source region.

Numerical simulations are useful tools for analyzing tsunami propagation and coastal amplification. The tsunami waves generated by earthquakes depend on the size and the impact of the source mechanism on the displaced water. Despite differences in the underlying physics of wave propagation in the sea and solid earth, the tsunami wave field emanating from an earthquake source can be thought of, as an extension to the seismic wave field (Okal, 1982).

There are at least three kinds of tsunami propagation and inundation models in common use among tsunami scientists: nonlinear shallow-water models (NSWMs), Boussinesq-type long-wave models, and complete fluid dynamics models, which all stem from the work of Peregrine (1967). NSWMs possess some distinctive advantages that make them very suitable for modeling flows occurring in shallow depths (Brocchini et al., 2001). We perform our study with the nonlinear shallow-water wave model. Since tsunami wavelengths are much larger than the sea depth, tsunamis are considered as shallow-water waves following the long-wave theory.

Long-wave theory is used (where the ratio of water depth to wavelength is small), for which the vertical acceleration of water particles is negligible compared with the gravitational acceleration, and the hydrostatic pressure approximation is used. The nonlinear terms are kept for their use where needed, which is the case in very shallow water (from the tsunami point of view). In addition, we are interested in this investigation on near-field tsunamis, that is, those whose propagation distance is less than 200 km. Henceforth Cartesian coordinates can be used. The vertical integrated governing equations (Dean and Dalrymple, 1984) can be written (after setting the momentum correction factors equal to unity, with Coriolis effect omitted):

$$\frac{\vartheta M}{\vartheta t}+\frac{\vartheta}{\vartheta \chi}\left(\frac{M^2}{D}\right)+\frac{\vartheta}{\vartheta y}\left(\frac{MN}{D}\right)+gD\frac{\vartheta \eta}{\vartheta \chi}+\frac{gk^2}{D^{7/3}}M\sqrt{M^2+N^2}=0 \quad (1)$$

$$\frac{\vartheta N}{\vartheta t}+\frac{\vartheta}{\vartheta \chi}\left(\frac{N^2}{D}\right)+\frac{\vartheta}{\vartheta y}\left(\frac{MN}{D}\right)+gD\frac{\vartheta \eta}{\vartheta \chi}+\frac{gk^2}{D^{7/3}}N\sqrt{M^2+N^2}=0 \quad (2)$$

$$\frac{\vartheta \eta}{\vartheta t}+\frac{\vartheta M}{\vartheta \chi}+\frac{\vartheta N}{\vartheta y}=0\,, \quad (3)$$

where η is the water surface elevation, *t* is time, *x* and *y* are the horizontal coordinates in zonal and meridional directions, and *M* and *N* are the discharge fluxes in the horizontal plane along *x* and *y* coordinates given by:

$$M=U(h+\eta)=UD \quad (4)$$

$$N = V(h+\eta) = VD \qquad (5)$$

where U and V are the vertically averaged horizontal particle velocities and $D=h(x, y)+\eta$ is the total water depth, $h(x, y)$ is the undisturbed basin depth, g is the gravity acceleration, and k is the bottom friction coefficient. For the simulation reported here and considering the prevailing bottom morphological features, k has been set equal to 0.025 (Fujima 2001).

For tsunami propagation, the numerical model employed in this study was developed by N. Shuto and F. Imamura, namely the Numerical Analysis Model for Investigation of Near field Tsunamis version 2 (TUNAMI-N2). This is one of the key tools for the developing studies for propagation and coastal amplification of tsunamis in relation to different initial conditions. It solves nonlinear shallow water equations in Cartesian coordinates using the leap-frog scheme of finite differences. Also, a similar methodology is used in the numerical model of the method of splitting tsunami (MOST) developed by Titov and Synolakis (1998). These are the only two existing nonlinear shallow water codes, validated with laboratory and field data (Yeh et al., 1996).

In this investigation, we use bathymetric data at a grid size of 87m. The total number of grid points in the computational domain was 8055799 consisting of 2741x2939 points. The time step is selected as 0.28sec to satisfy the CFL stability condition (e.g. Tselentis et al., 2006; Goto and Ogawa, 1992). The duration time of wave propagation was 60minutes.

Our simulations have two classes of products: we first compute snapshots of the sea surface displacement all over the grid at time intervals of 4min. Second, we compute time series of water surface elevations (mareograms or virtual gauges) at eleven selected locations along the Ionian shorelines possessing increased tsunami hazard due to recent tourist development.

Discussion of the results

Fig.3 presents snapshots of the water surface displacement at 4 minutes interval up to 20 minutes, for Filiatra fault (source 1) and Fig.5 presents the corresponding mareograms at

12 most important tourist resorts along the Ionian shoreline (Fig. 4). This potential tsunami source is an off-shore fault recognised from a 'clustering' of the seismicity; it has a NNW SSE direction almost parallel to the nearby Peloponnesus coast, and it is a thrust fault with length L=70km and width W=45km (Papazachos and Papazachou, 1997, Papanikolaou et al., 2007). Several moderate to strong earthquakes have been attributed to this fault; in 1886 this was the source of a magnitude 7.5 event (estimated from the observed maximum intensity of XM), also the 1899 Kyparissia (M=6.5; Papazachos and Papazachou, 1997) and the 1919 Kyparissia (M=6.3; Papazachos and Papazachou, 1997) earthquakes, have been related with this fault.

As we can see from Fig. 3 after 4 minutes the wave arrives at Pilos city coastal area, where it reaches a maximum amplitude of 1.6m after 6min. After 8min, the wave arrives at Proti island where it reaches the greatest amplitude observed in this simulation, 4m at 16min. For this reason we focus in this area, depicting tsunami propagation snapshots at higher magnification.

After 9 minutes, the wave arrives at the tourist resort of Laganas bay in Zakynthos, where it reaches a maximum amplitude of 3.5m after 11min. This is a heavily populated region during the summer with thousands of tourists in the coastal zone and needs specific attention and tsunami risk reduction planning.

For all the rest locations, wave amplitudes are relatively small with the exception of Kyparisia region where 13min and 19min after the activation of the fault it reaches an amplitude of 3m. This is also a heavily populated tourist area during Summer time.

Fig.6 shows snapshots of the tsunami propagation corresponding to the activation of the Zakynthos fault (source 2). The corresponding mareogramas at the locations depicted in Fig.4 are presented in Fig.7. This potential source is mapped according to seismological evidence (FAUST database) proposed by Ambraseys and Jackson (1990) on the base of the 1958 earthquake with magnitude M=7.0. It is a thrust fault with length L=35km and width W=22km. The focal mechanism adopted by the FAUST database is in consistency with focal mechanisms calculated from recent earthquakes located in the area South of Zakynthos.

Judging from the above figures, we can see that the activation of this particular source has little effect on the tsunami hazard of the region under investigation. The greatest wave amplitudes are reached at Kyparisia bay where they become 1m at 16, 21 and 25 minutes after the source activation. Also at the Lagana bay region, they reach an amplitude of 0.9m 7min after the activation of the source.

Fig.8 shows snapshots of the tsunami propagation corresponding to the activation of the Cephalonia South fault (source 3). The corresponding mareogramas at the locations depicted in Fig.4 are presented in Fig.9. This source is located in the sea area North of Zakynthos island. According to Monopolis and Bruneton (1982) the northern flank of Zakynthos is steep and is affected by large normal faulting. It is suggested that this normal fault caused the 1554 earthquake, while the maximum expected magnitude from this source is M=6.5 (Stucchi et al., 2001).

In this case we see that the activation of Cephalonia South source possesses no significant tsunami hazard in the region, since all the wave amplitudes are below 0.5m. The greatest amplitude is observed at Laganas bay, where it becoms 0.4m.

Source 3 and source 4 (Cephalonia South and North faults) are mapped in Fig.1 according to Lagios et al., 2007, where it is mentioned that major faults having length of several tenths of kilometers in the marine area between Cephalonia and Zakynthos could control the tectonic movements in the area. Source 4 represents a normal fault, which is located in the coastal area of Cephalonia. The fault dimensions where computed according to empirical relationships (Papazachos and Papazachou, 1997). FAUST database (after Stucchi et al., 2001) suggests this source as the causative fault of the 1636 earthquake (M=7.1).

Fig.10 shows snapshots of the tsunami propagation corresponding to the activation of the Cephalonia North fault (source 4). The corresponding mareograms at the locations depicted in Fig.4 are presented in Fig.11.

Judging from the above figures we can see that the results obtained are similar to those corresponding to the activation of source 3. The greatest wave amplitude is 0.5m and is reached at Laganas bay at 20 and 28 minutes after the source activation.

Conclusions

The main objective of this work was the study of possible tsunamis in the Ionian Sea. This was carried out by using a forward modeling approach, that is, by running numerical tsunami simulations, relative to different genetic mechanisms that seem plausible on the basis of the present knowledge of the seismotectonics of the region.

Special emphasis was given at eleven tourist resorts, where we computed the corresponding for the activation of each of the four sources, mareograms. From all the examined sources only source 1 possesses serious threat causing wave propagation amplitude reaching up to 4m at two locations. Since these locations are heavily populated during summer time, the need for special tsunami risk mitigation measures is obvious.

References

Ambraseys, N.N., The seismic sea wave of July 9, 1956, in the Greek Archipelago. Journal of Geophysical Research, Vol. 65, No. 4, p. 1257-1265, 1960.

Ambraseys, N.N., Data for the Investigation of the Seismic Sea Waves in the Eastern Mediterranean. Bull. Seis. Soc. Amer., Vol. 52, No. 4, 895-913, 1962.

Ambraseys N.N. and Jackson J.A., Seismicity and associated strain of central Greece between 1890 and 1988. Geophys. J. Int., 101, 663-708, 1990.

Antonopoulos, J. A., Data from the investigation of seismic sea-wave events in the eastern Mediterranean from the birth of Christ to 1980 AD (six parts), Ann. Geophys. 33, 141–248, 1980.

Antonopoulos, J. A., Tsunamis of Eastern Mediterranean from Antiquity until Today, Athens (in Greek), 1973.

Brocchini, M., Bernetti, R., Mancinelli, A. and Albertini, G.: An efficient solver for nearshore flows based on the WAF method, Coastal Eng. 43, 105–129, 2001.

Comer, R. P.: Tsunami generation: a comparison of traditional and normal mode approaches, Geophys. J. R. Astr. Soc. 77, 29-41, 1984.

Dean, R. G., and Dalrymple, R. A.: Water Wave Mechanics for Engineers and Scientists,World Scientific Publishing Co., Singapore, 353 pp, 1984

DeMets, C., Gordon, R. G., Argus, D. F., and Stein, S.: Current plate motions, Geophys. J. Int., 101,425-478, 1990.

Fujima, K.: Long wave propagation on large roughness, ITS Proceedings, Session 7, no. 7-22, 891–895, 2001

Galanopoulos, A., La sismicité de l'Achaie et des régions voisines de Missolonghi et de Naupacte, Gerl. Beitr. Geophys., vol. 53, Leipzig, 1938.

Galanopoulos, A., Die Seismizität der Insel Leukas; Allgemeine historische Uebericht, Gerl. Beitr. Geophys., vol. 62, Nr. 4, Leipzig, 1952.

Galanopoulos, A., A catalogue of shocks in Greece with I -> VI or M > 5 for the years 1801 to 1958, Publications, Seismological Laboratory, University of Athens, Athens, 1960.

Galanopoulos, A., A catalogue of shocks in Greece with i >= VII for the years prior to 1800, Publications, Seismological Laboratory, University of Athens, Athens, 1961.

Geist, E.L.: Local tsunamis and earthquake source parameters, in Tsunamigenic Earthquakes and Their Consequences, Adv. Geophys, Academic Press, San Diego, 39, 117-209, 1998

Geist, E.L., and Parsons, T.: Probabilistic analysis of tsunami hazards, Natural Hazards 37, 277-314, 2006.

Goto, C., and Ogawa, Y.: Numerical method of tsunami simulation with the leap-frog scheme, Dept. of Civil Engineering, Tohoku University, Translated from TIME project by N. Shuto, 1992

Goto, C., Ogawa, Y., Shuto, N., and Imamura, N.: Numerical method of tsunami simulation with the leap-frog scheme (IUGG/IOC Time Project), IOC Manual. United Nations Educational Scientific and Cultural Organization (UNESCO), No. 35, 1997.

Haslinger, F., Kissling, E., Ansorge, J., Hatzfeld, D., Papadmitriou, E., Karakostas, V., Makropoulos, K., Kahle, H-G., Peter, Y.: 3D crustal structure from local earthquake tomography around the Gulf of Arta (Ionian region, NW Greece), Tectonophysics, 304, 201-218, 1999.

Hoff, K., Chronik der Erdbeben und Vulkan-Ausbrüeche, mit vorausgehender Abhandlung über die Natur dieser Erscheinungen, Gesch. Ueberlieferung nachgew natürl. Veränder. Erdoberfläche, Parts 4 and 5, Gotha, 1841.

Jackson, J., and McKenzie, D.: Rates of active deformation in Aegean Sea and surrounding regions, Basin Research, 1, 121-128, 1988.

Jackson, J., Active tectonics of the Aegean region, Annu. Rev. Earth Planet. Sci., 22, pp, 239–271, 1994.

Kahle, H.-G., Müller, M.V., Mueller, S., Veis, G., Billiris, H., Paradissis, D., Drewes, H., Kaniuth, K., Stuber, K., Tremel, H., Zerbini, S., Corrado, G. and Verrone, G.: Monitoring West Hellenic Arc Tectonics and Calabrian Arc Tectonics (‘WHAT A CAT') using the Global Positioning System, In: Smith, D., Turcotte, D. (Eds.), Contribution of Space Geodesy to Geodynamics, AGU Geodyn. Ser., 23, 417–429, 1993.

Legg, M. R., Eeeri, M., Borrero, J. C. and Synolakis, C. E.: Tsunami hazards associated with the Catalina fault in Southern California, Earthquake Spectra 20, no. 3, 917–950, 2004.

Liu, P.L., Synolakis, C.E., and Yeh, H.: Impressions from the First International WorkShop on Long Wave Runup, J. Fluid Mech., 229, 675-688, 1991.

Liu, Y., Santos, A., Wang, M.S., Shi, Y., Liu, H., and Yuen, D.: Tsunami hazard along Chinese coast from potential earthquakes in South China Sea, Phys. Of the Earth and Plan. Inter., 163, 233-244, 2007.

Makropoulos, C., and Burton, P.W.: A catalogue of the seismicity in Greece and adjacent areas, Geophys. J.R.Astr. Soc., 65, 741-762, 1981.

Mallet, R., Report on the facts of earthquake phaenomena, British Assoclarion for the Advancement of Science, Part 1, 1850 pp. 89, Part 2, 1852 pp. 212, Part 3,1854 pp., 326, Part 4, 1858 pp., 136, Published by J. Taylor, 1850-1858.

Mansinha, L. and Smylie, D. E.: The displacement fields of inclined faults, Bull. Seism. Soc. Am., 61, 1433-1440, 1971.

Mariolakos, I., Papanikolaou, D., and Lagios, E.: A neotectonic geodynamic model of Peloponnese based on morphotectonics, repeated gravity measurements and seismicity, Geol. Jb, B50, 3–17, 1985.

Monopolis, D. and Bruneton, A. Ionian Sea (Western Greece): its structural outline deduced from drilling and geophysical data, Tectonophysics 83, 227–242, 1982.

Noomen, R., Springer, T., Ambrosius, B., Herzberger, K., Kuijper, D., Mets, G., Overgaauw, B. and Wakker, K.: Crustal deformations in the Mediterranean area computed from SLR and GPS observations, J. Geodyn., 21 1, 73–96, 1995.

Okada, Y.: Surface deformation due to shear and tensile faults in half space, Bull. Seism. Soc. Am., 75, 1135–1154, 1985.

Okal, E. A.: Mode-wave equivalence and other asymptotic problems in tsunami theory, Phys. Earth. Planet. Interiors, 30, 1–11, 1982.

Ornstein, B., Das Erdbeben fon Vostiza Ausland, vol. 62, p. 453, München-Stuttgart, 1889.

Papanikolaou D., Fountoulis I., Metaxas C.: Active faults, deformation rates and Quaternary paleogeography at Kyparissiakos Gulf (SW Greece) deduced from onshore and offshore data, Quaternary International, 171-172, (SPEC. ISS.), 14-30, 2007.

Papazachos, B. C., Koutitas, Ch., Hatzidimitriou, P. M., Karacostas, B. G., and Papaioannou, Ch. A., Source and short-distance propagation of the July 9, 1956 southern Aegean tsunami, Marine Geol. 65, 343–351,1985.

Papazachos, B. C., Koutitas, Ch., Hatzidimitriou, P. M., Karacostas, B. G., and Papaioannou, Ch. A., Tsunami hazard in Greece and the surrounding area, Ann. Geophys. 4, 79–90, 1986.

Papazachos, B.C. and Dimitriu, P.P., Tsunamis in and near Greece and their relation to the earthquake focal mechanisms, Natural Hazards 4, 161-170, 1991.

Papazachos, B., Kiratzi, A. and Papadimitriou, E.: Regional focal mechanisms for earthquakes in the Aegean Area, Pure Appl. Geophys, 136, 407–420, 1991.

Papazachos, B., and Papazachou, C.: Earthquakes in Greece. Ed. Ziti, Thessaloniki, 1997.

Peregrine, D.H.: Long waves on a beach. J. Fluid Mech. 27, 815–827, 1967.

Satake, K., and Somerville, P.G.: Location and size of the 1927 Lompoc, California, earthquake from tsunami data, Bull. Seismol. Soc. Am., 82, 1710-1725, 1992.

Sieberg, A., Untersuchungen über Erdbeben und Bruchschollenbau im östlichen Mittelmeergebiet" Denkschriften der Medizinisch~Naturwissenschaftlichen Gesellschafl zu Jena, vol. 2, Jena, 1932.

Soloviev, S. L., Solovieva, O.N., Go, C. N., Kim, K. S., and Shchetnikov, N. A., Tsunamis in the Mediterranean Sea 2000 B.C.-2000 A.D., Advances in Natural and Technological Hazards Research, Volume 13, Kluwer Academic Publishers, Dordrecht, Netherlands, 237 p, 2000.

Stucchi, M., Albini, P., Camassi, R., Musson, R.M.W and Tatevossian, R. Main results of the Project BEECD “A Basic European Earthquake Catalogue and a Database for the Evaluation of Long-term Seismicity and Seismic Hazard”. In: M. Yeroyanni, C. Margottini and G. Zonno, Editors, Tools for planning in seismic areas: integrated approaches and data availability, European Commission Volume, Brussels, 2001.

Taymaz, T., Jackson, J.A. and Westway, R.: Earthquake mechanisms in the Hellenic Trench near Crete, Geophys. J. Int., 102, 695–732, 1990.

Thomas, A.M.: Poly 3D: a three-dimensional, polygonal element, displacement discontinuity boundary element computer program with applications to fractures, faults and cavities in the Earth's crust, MSc Thesis, Stanford University, 1993.

Titov, V.V. and Synolakis, C.E.: Numerical modeling of tidal wave runup, Journal of Waterways, Port, `Coastal and Ocean Engineering, ASCE, 124, 4, 157-171, 1998.

Tselentis, G-A., Gkika, F., and Sokos, E.: Tsunami hazards associated with the Perachora fault at eastern Corinth gulf, Greece, Bull. Seism. Soc. Am., 96,5, 1649-1661, 2006.

Vidal, L., Sur le tremblement de terre du 27 Aoflt 1886 en Grece, Comptes Rendus de l'Acaddmie de Sciences, vol. 103, Paris, 1886

Yeh.H., Liu. P., and Synolakis, C. (Eds) : Long-wave run-up models, Proceedings of the international workshop, Friday Harbor, USA,1995, World Scientific publishers Co, Singapore, 1996.

CAPTIONS OF TABLES

Table 1: Possible, locally generated, tsunami along the western Hellenic arc fault system. K_o is the intensity of the wave and it refers to Sieberg's modified intensity scale (1932).

Table 2: Fault parameters of the selected potential tsounamigenic sources used for the numerical simulation.

Table 3: Sea bottom deformations due to the activation of the four potential sources.

CAPTIONS OF FIGURES

Fig.1: Earthquakes with M>6 occurred along the Ionian Sea and the potential tsounamigenic sources considered in the present investigation; contour depths are in km. Stars, denote earthquake epicenters possibly related with tsunami.

Fig.2: E deformation of sea bottom due to the activation of the four sources considering the source parameters depicted in Table 2.

Fig.3: Snapshots of the tsunami propagation from the source 1 (Filiatra fault) at 4-min interval. The propagation close to Proti islet is presented in the last row, at a higher magnification.

Fig.4: Locations of the gouges considered in the present investigation which represent the most populated tourist resorts along the Ionian shoreline.

Fig.5: Calculated mareograms at the locations shown in Fig.4, for source 1 (Filiatra fault).

Fig.6: Snapshots of the tsunami propagation from the source 2 (Zakynthos fault) at 4-min interval.

Fig.7: Calculated mareograms at the locations shown in Fig.4, for source 2 (Zakynthos fault).

Fig.8: Snapshots of the tsunami propagation from the source 3 (Cephalonia South fault) at 4-min interval.

Fig.9: Calculated mareograms at the locations shown in Fig.4, for source 3 (Cephalonia South fault).

Fig.10: Snapshots of the tsunami propagation from the source 4 (Cephalonia North fault) at 4-min interval.

Fig.11: Calculated mareograms at the locations shown in Fig.4, for source 4 (Cephalonia North fault).

No	Year	Month	Day	Lat Lon	Region	M	Ko	References
1	1622	05	05	37.60 21.00	Zakynthos Is., Ionian Sea	6.6	-	Ambraseys, 1960, Galanopoulos, 1960, Antonopoulos, 1980
2	1633	11	05	37.70 20.80	Zakynthos Is., Ionian Sea	7,0	2	Ambraseys, 1962, Papazachos and Dimitriu, 1991, Papazachos et al., 1985, Papazachos et al., 1986, Antonopoulos, 1973
3	1636	09	30	38.10 20.30	Kefalonia	7.2	3	Papazachos & Dimitriu, 1991, Papazachos et al., 1985,Papazachos et al., 1986, Antonopoulos, 1973
4	1723	02	22	38.60 20.65	Lefkada	6.7	2+	Ambraseys, 1962, Galanopoulos,1961, Papazachos & Dimitriu, 1991, Papazachos et al., 1985
5	1732	11		39.40 20.10	Corfu	6.5	2	Ambraseys, 1962,Papazachos & Dimitriu, 1991, Papazachos et al., 1985,Papazachos et al., 1986, Antonopoulos, 1973
6	1791	11	02	37.90 21 00	Zakynthos Is., Ionian Sea	6.8	3	Ambraseys, 1962, Mallet,1850-1858 Papazachos & Dimitriu, 1991, Papazachos et al., 1985,
7	1804	06	08	38.10 21.70	Patras Gulf	6.4	3	Ambraseys, 1962, Hoff, 1841, Galanopoulos,1960, Papazachos & Dimitriu, 1991
8	1805	01	08	38.30 21.80	Patras Gulf		-	Ambraseys, 1962, Hoff, 1841, Galanopoulos,1960, Papazachos & Dimitriu, 1991

9	1820	03	17	38.80 20.80	Lefkada		-	Soloviev et al., 2000
10	1820	12	29	37.80 21.10	Zakynthos Is., Ionian Sea	6.9	3+	Papazachos & Dimitriu, 1991, Papazachos et al., 1985, Papazachos et al., 1986, Antonopoulos, 1973
11	1821	01	09	38.15 21.59	Patras Gulf		4	Ambraseys, 1962, Mallet,1850-1858, Galanopoulos,1938
12	1825	01	19	38.70 20.60	Ionian Sea	6.8	3	Soloviev et al., 2000,26
13	1835	07	12	37.70 21.10	Zakynthos Is., Ionian Sea		2	Ambraseys, 1962, Antonopoulos,1980
14	1867	02	04	38.39 20.52	Kefalonia	7.4	2	Papazachos & Dimitriu, 1991, Papazachos et al., 1985, Papazachos et al., 1986, Antonopoulos, 1973
15	1867	04	10	38.20 20.44	Lixouri, Kefalonia		2	Ambraseys, 1960, Soloviev et al., 2000
16	1869	12	28	38.85 20.80	Lefkada	6.4	2	Ambraseys, 1962, Galanopoulos,1952
17	1883	06	27	39.50 20.00	Ionian Sea		3	Ambraseys, 1962, Galanopoulos,1960, Antonopoulos,1980, Soloviev et al., 2000
18	1886	08	27	37.00 21.40	W.Filiatra	7.5	3	Ambraseys, 1962, Vidal, 1886, Ornstein, 1889, Galanopoulos,1960, Galanopoulos,1960b
19	1889	01	22	37.20	Gulf of	6.6	3	Papazachos & Dimitriu, 1991, Papazachos et al., 1985,

				21.60	Kyparissia			Papazachos et al., 1986, Antonopoulos, 1973
20	1893	04	17	37.68 20.81	Zakynthos Is., Ionian Sea	6.4	2	Ambraseys, 1960
21	1897	12		37.80 21.00	Ionian Sea			Antonopoulos,1980
22	1898	12	03	37.80 21.00	Ionian Sea		3	Ambraseys, 1962, Antonopoulos,1980, Soloviev et al., 2000
23	1899	01	22	37.20 21.60	Kyparissia	6.5	3	Ambraseys, 1962, Mitzopoulos, 1900,
24	1914	11	27	38.72 20.62	Lefkada	6.3	4	Ambraseys, 1962, Galanopoulos,1952, Papazachos & Dimitriu, 1991
25	1915	08	07	38.50 20.62	Lefkada	6.7	3	Ambraseys, 1962, Galanopoulos,1960, Galanopoulos,1952, Papazachos & Dimitriu, 1991
26	1947	10	06	36.96 21.68	W.Pylos, Methoni	7.0	3	Ambraseys, 1962, Galanopoulos,1952, Papazachos & Dimitriu, 1991
27	1948	04	22	38.71 20.57	Lefkada Vassiliki	6.5	3	Ambraseys, 1962, Galanopoulos,1955, Galanopoulos,1960, Papazachos & Dimitriu, 1991

Table 1

Id	Fault Name	Type	Strike (deg)	Dip (deg)	Rake (deg)	Slip (cm)	Length (Km)	Width (Km)	Mw	Depth (Km)
1	Filiatra	thrust	329	30	121	275	70	45	7.5	2
2	Zakynthos	thrust	329	22	120	107	35	22	7	2
3	Cephalonia South	normal	270	60	-90	42	37	13	6.5	2
4	Cephalonia North	normal	110	60	-90	107	40	22	7.1	2

Table 2

Id	Fault Name	Vertical Calculated Displacement (cm) (Poly3D)	
		Min (Βύθιση)	**Max (Ανύψωση)**
1	Filiatra	-19	135
2	Zakynthos	-12	39
3	Cephalonia South	-56	7
4	Cephalonia North	-67	8

Table 3

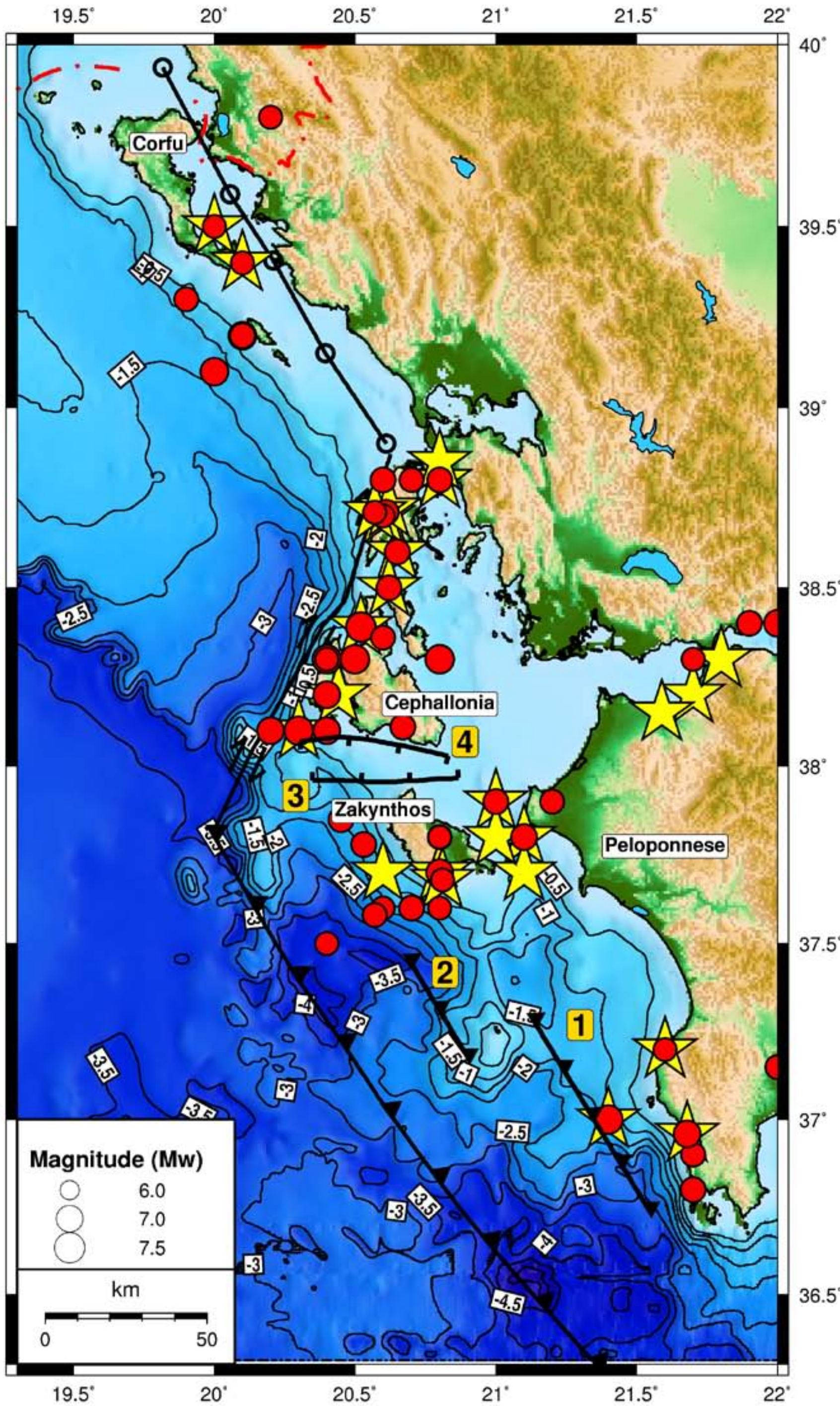

19.5°
20°
20.5°
21°
21.5°
22°
40°
39.5°
39°
38.5°
38°
37.5°
37°
36.5°
Corfu
Cephallonia
Zakynthos
Peloponnese
1
2
3
4
Magnitude (Mw)
6.0
7.0
7.5
km
0
50

FIG1

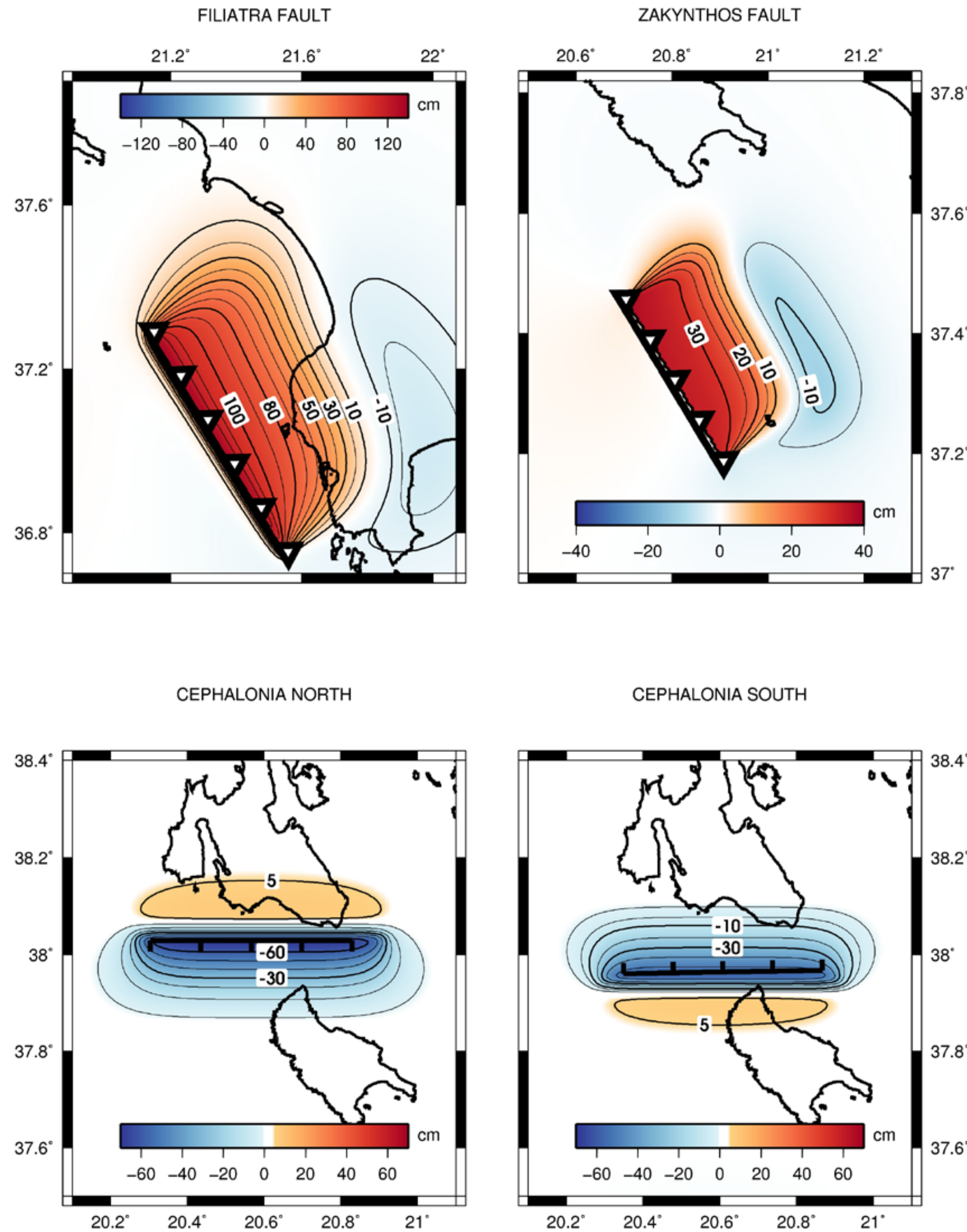
FILIATRA FAULT
ZAKYNTHOS FAULT
CEPHALONIA NORTH
CEPHALONIA SOUTH
cm
100
80
50
30
10
-10
30
20
10
-10
5
-60
-30
-10
-30
5

FIG2

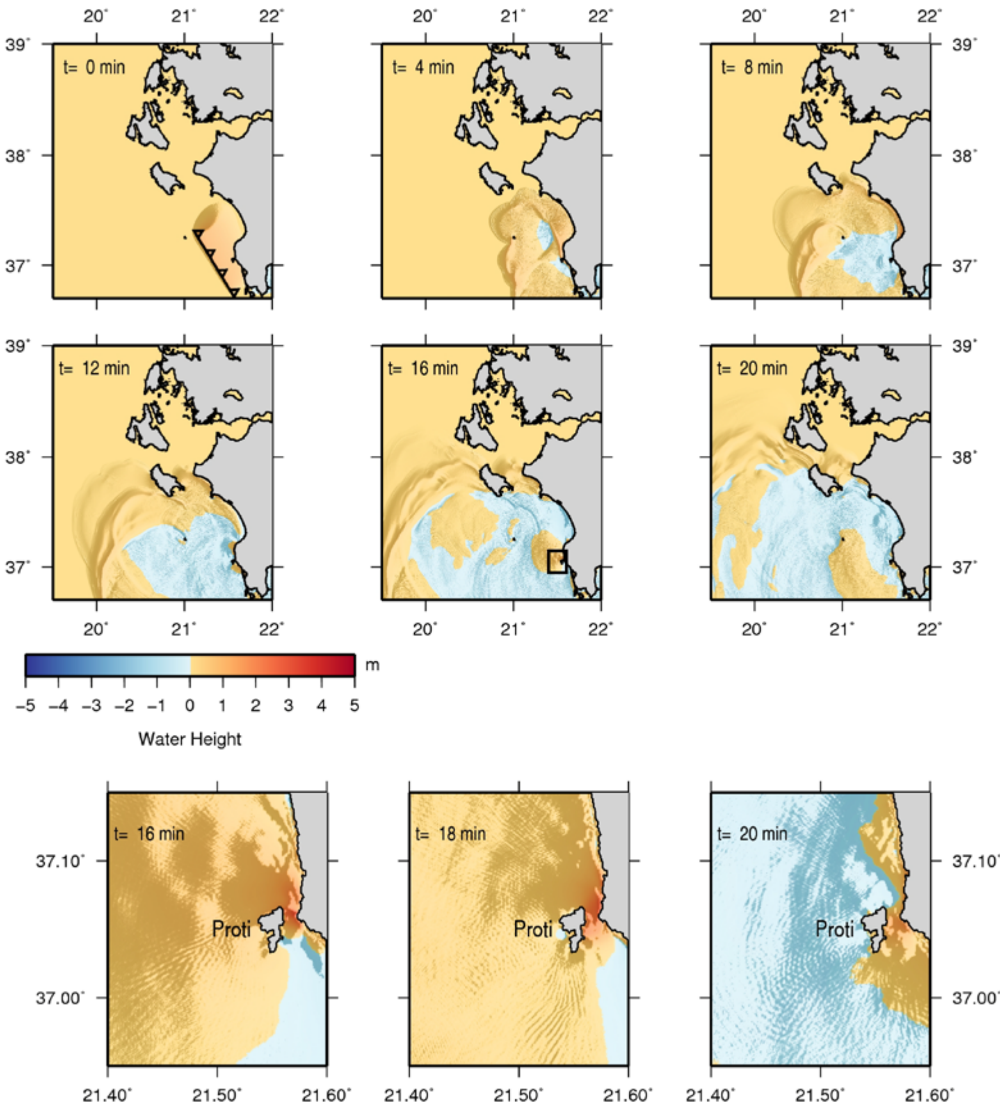

t= 0 min
t= 4 min
t= 8 min
t= 12 min
t= 16 min
t= 20 min
20˚
21˚
22˚
39˚
38˚
37˚
m
−5 −4 −3 −2 −1 0 1 2 3 4 5
Water Height
t= 16 min
t= 18 min
t= 20 min
Proti
37.10˚
37.00˚
21.40˚
21.50˚
21.60˚

FIG3

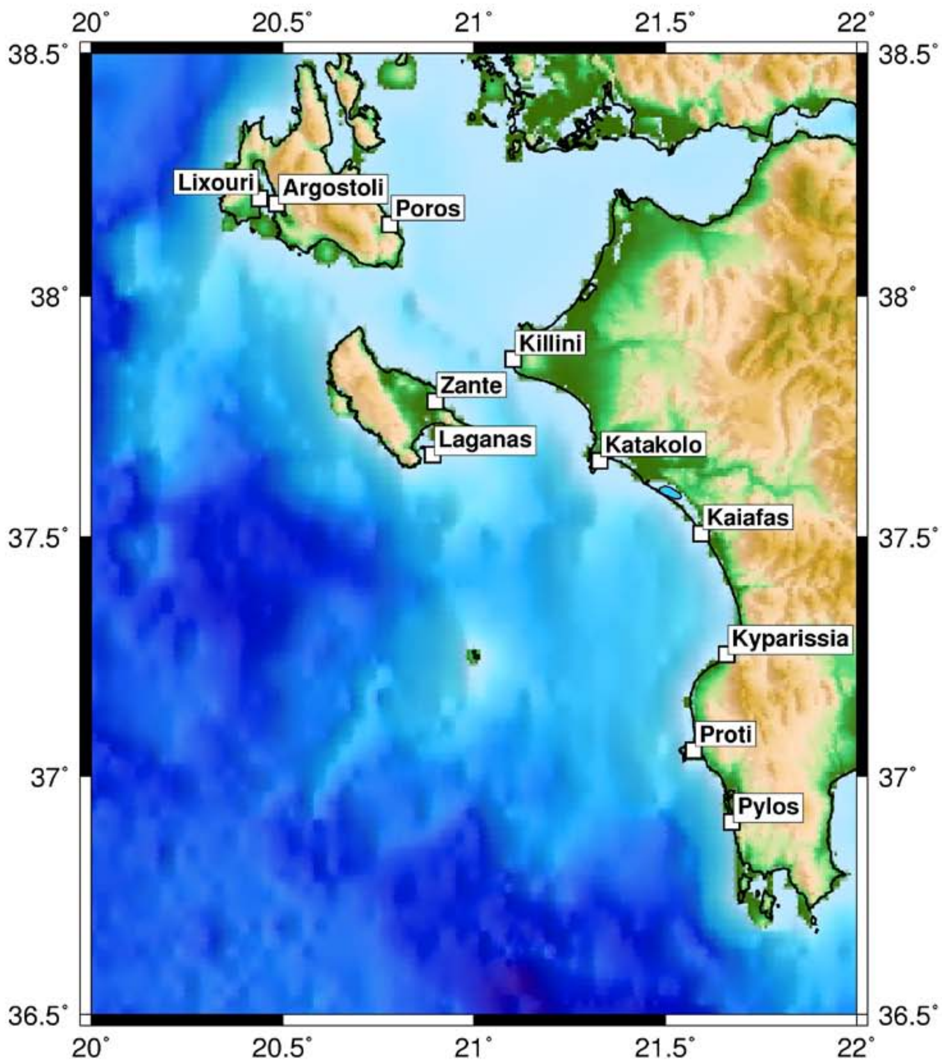
20˚
20.5˚
21˚
21.5˚
22˚
38.5˚
38˚
37.5˚
37˚
36.5˚
Lixouri
Argostoli
Poros
Killini
Zante
Laganas
Katakolo
Kaiafas
Kyparissia
Proti
Pylos

FIG4

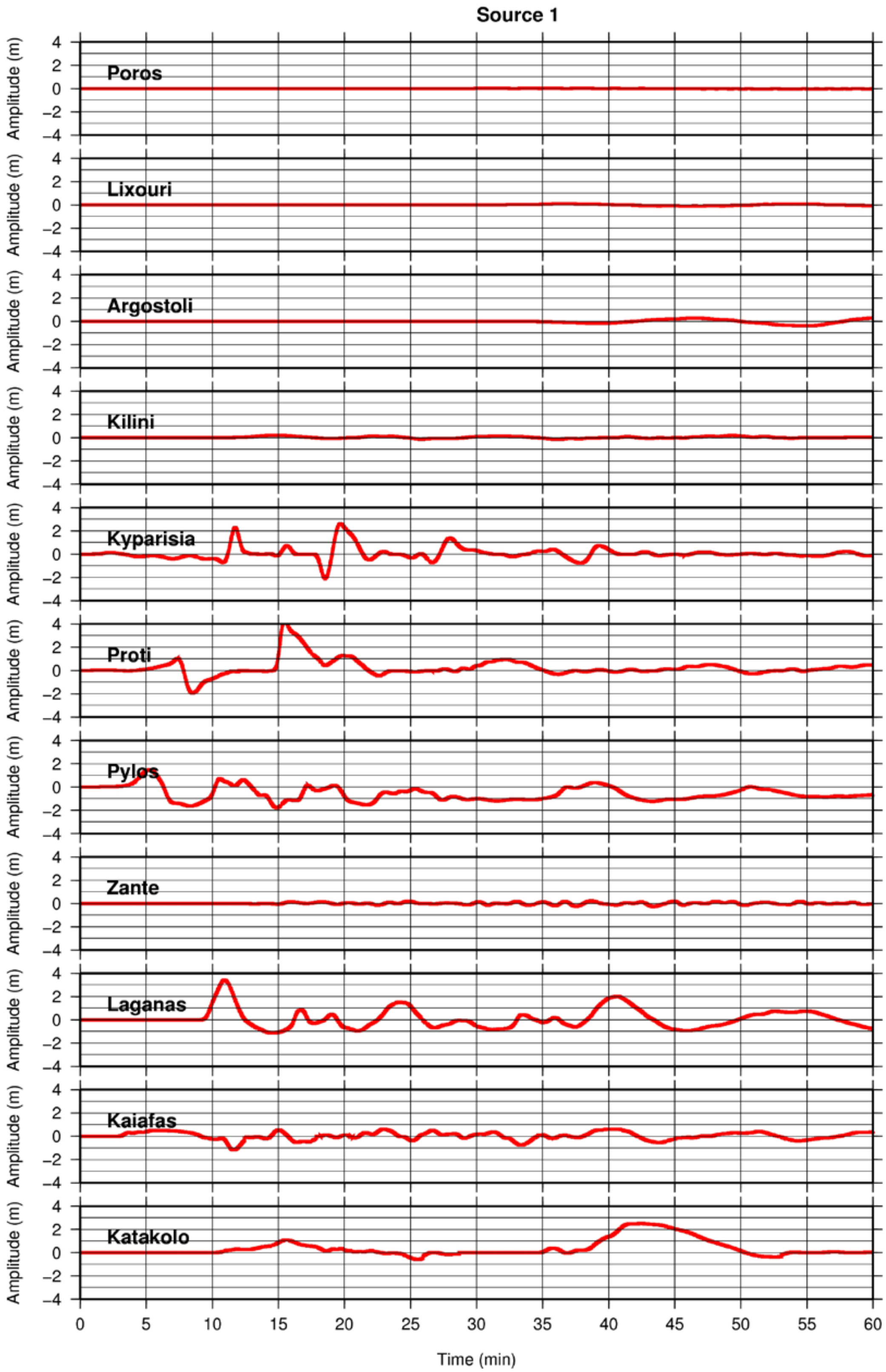
Source 1
Poros
Lixouri
Argostoli
Kilini
Kyparisia
Proti
Pylos
Zante
Laganas
Kaiafas
Katakolo
Amplitude (m)
Time (min)

FIG5

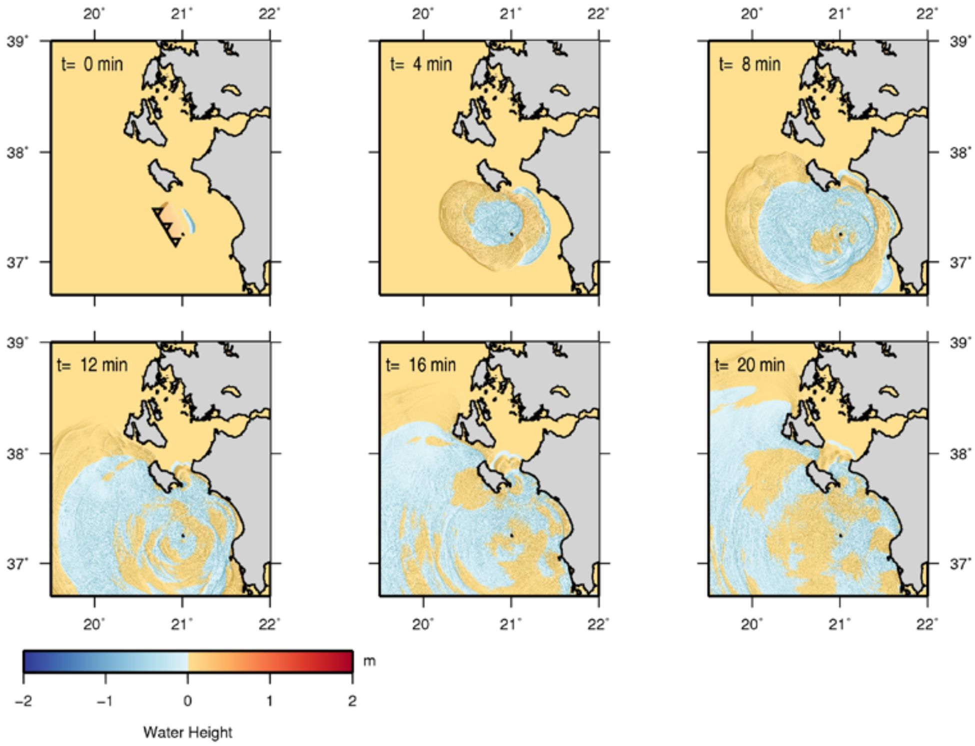
20°
21°
22°
39°
38°
37°
t= 0 min
t= 4 min
t= 8 min
t= 12 min
t= 16 min
t= 20 min
m
−2
−1
0
1
2
Water Height

FIG6

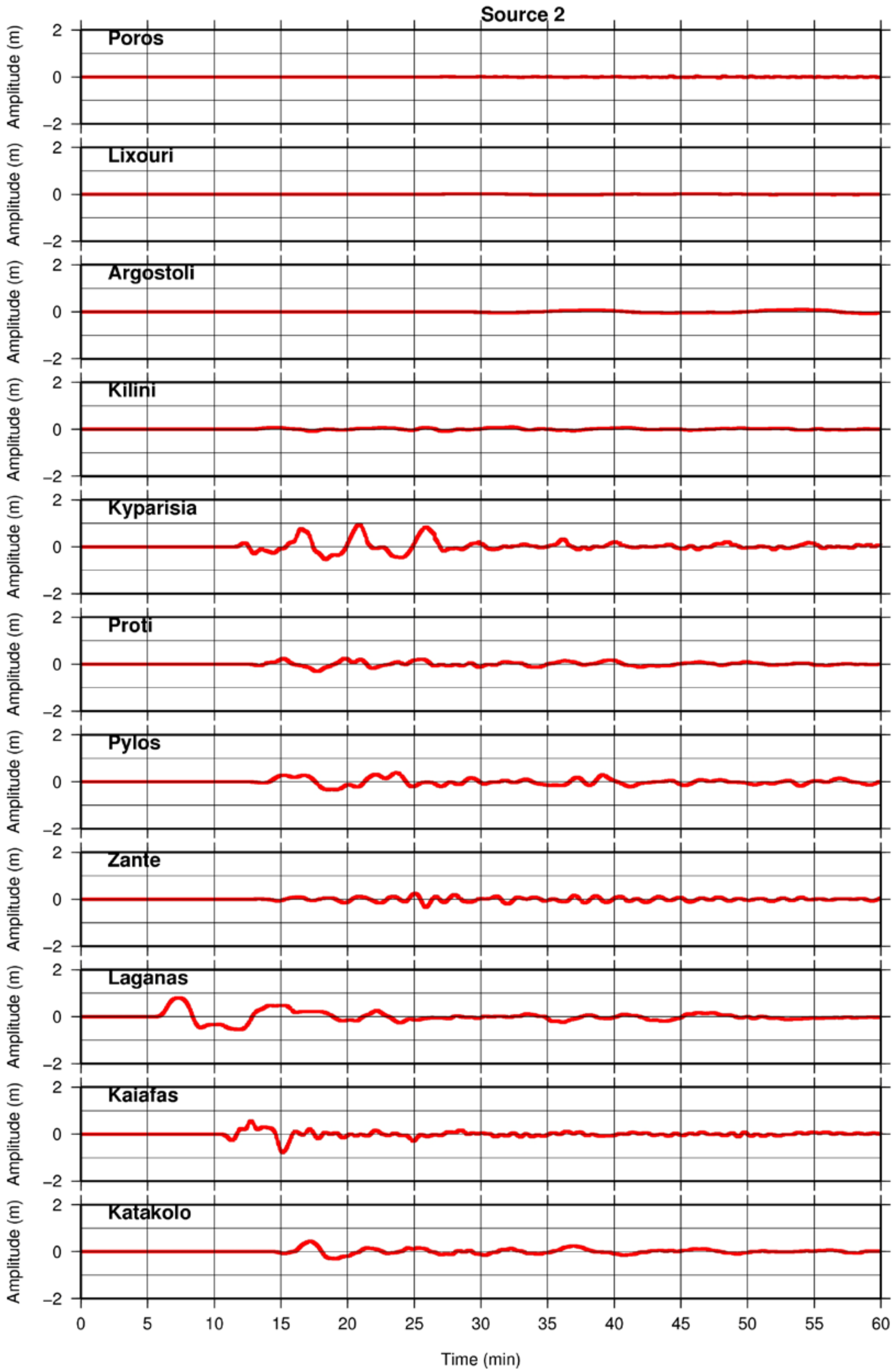

Source 2
Poros
Lixouri
Argostoli
Kilini
Kyparisia
Proti
Pylos
Zante
Laganas
Kaiafas
Katakolo
Amplitude (m)
2
0
−2
0
5
10
15
20
25
30
35
40
45
50
55
60
Time (min)

FIG7

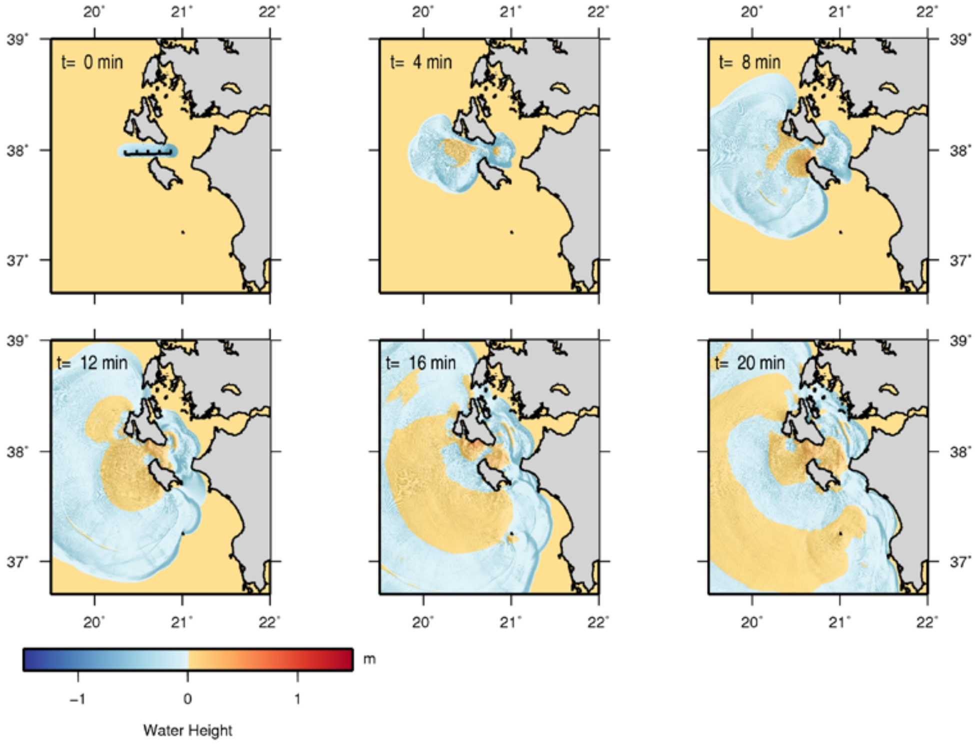
t= 0 min
t= 4 min
t= 8 min
t= 12 min
t= 16 min
t= 20 min
20°
21°
22°
39°
38°
37°
m
−1
0
1
Water Height

FIG8

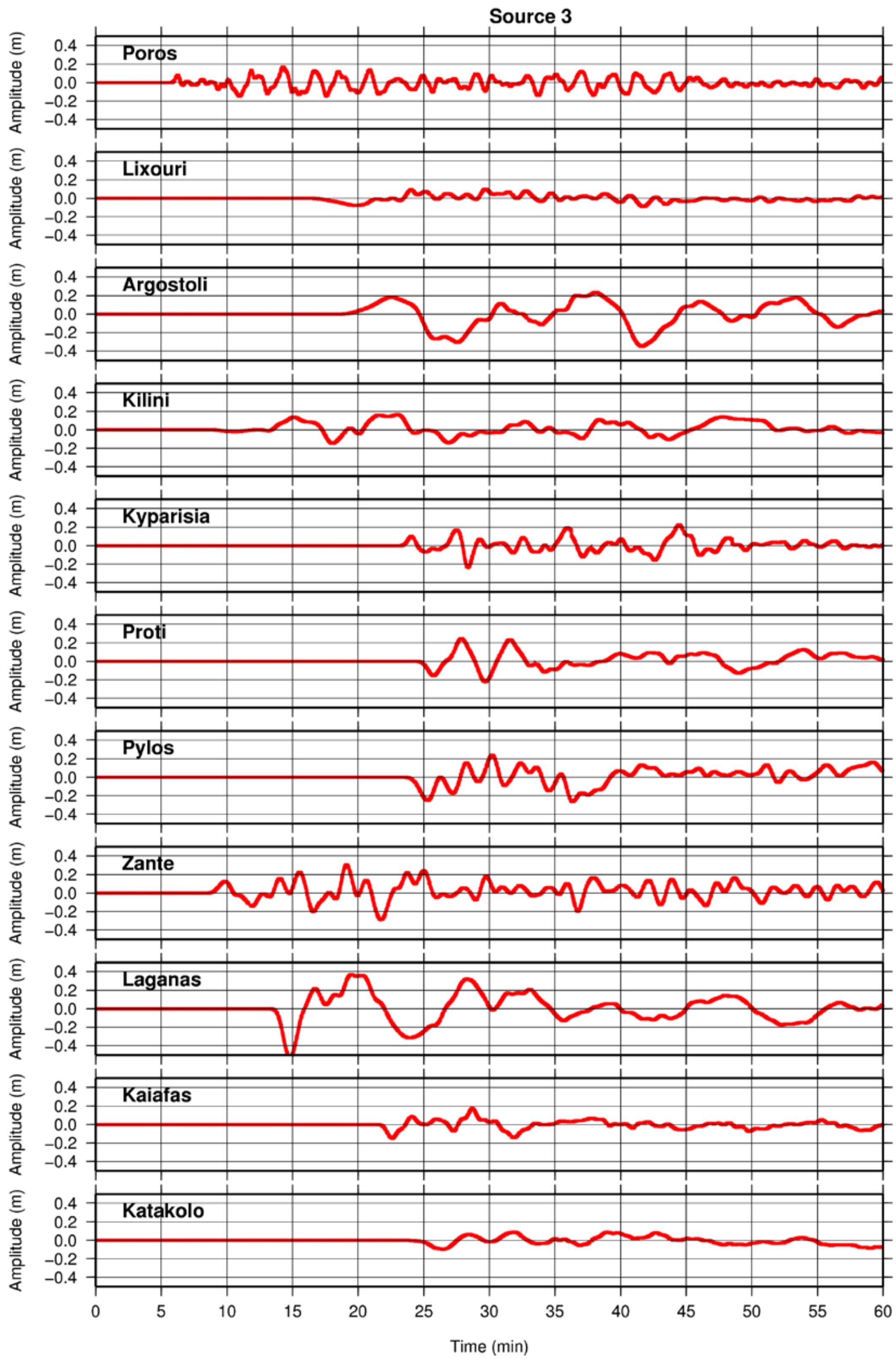
Source 3
Poros
Lixouri
Argostoli
Kilini
Kyparisia
Proti
Pylos
Zante
Laganas
Kaiafas
Katakolo
Amplitude (m)
Time (min)

FIG9

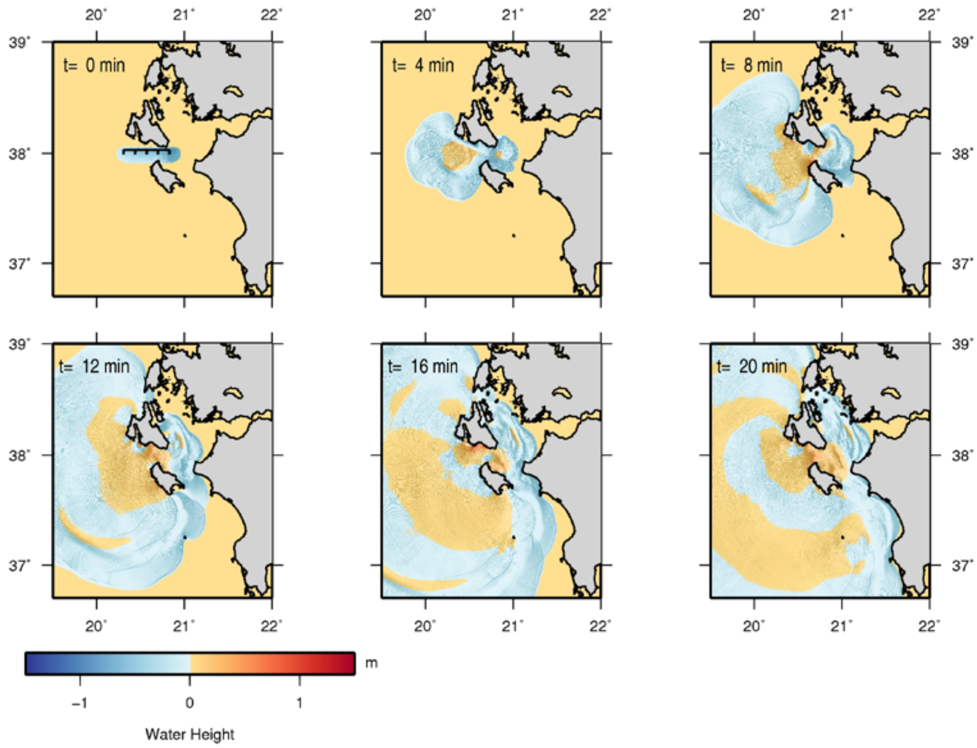
t= 0 min
t= 4 min
t= 8 min
t= 12 min
t= 16 min
t= 20 min
20°
21°
22°
39°
38°
37°
m
−1
0
1
Water Height

FIG10

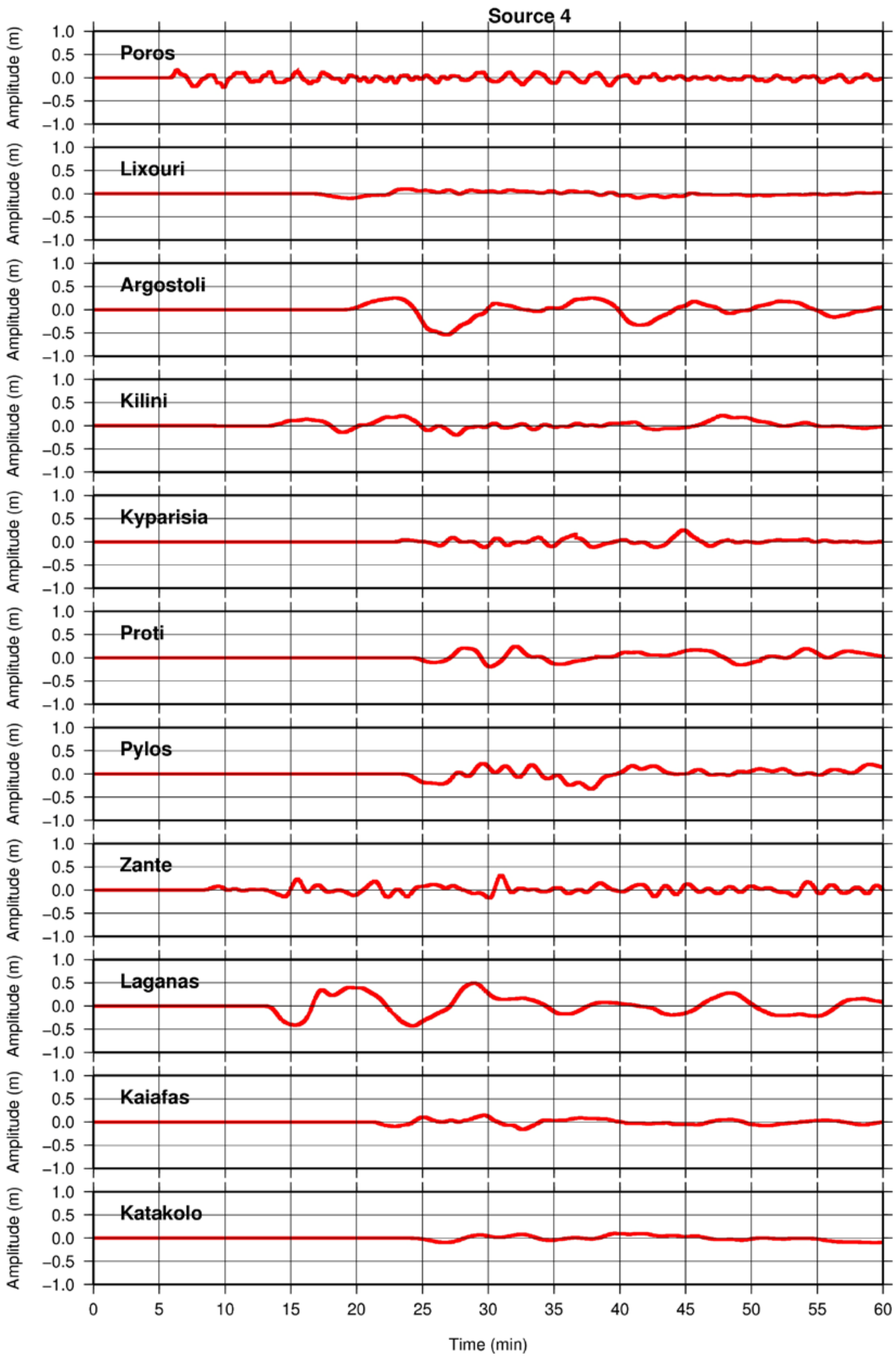
Source 4
Poros
Lixouri
Argostoli
Kilini
Kyparisia
Proti
Pylos
Zante
Laganas
Kaiafas
Katakolo
Amplitude (m)
1.0
0.5
0.0
−0.5
−1.0
0
5
10
15
20
25
30
35
40
45
50
55
60
Time (min)

FIG11